Article

2,6-Pyridodicarboxamide-bridged Triptycenes Molecular Transmission Devices: Converting Rotation to Rocking Vibration

Guangxia Wang, Lishuang Ma, JunFeng Xiang, Ying Wang, Xuebo Chen, Yanke Che, and Hua Jiang

J. Org. Chem., **Just Accepted Manuscript** • DOI: 10.1021/acs.joc.5b01778 • Publication Date (Web): 21 Oct 2015

2,6-Pyridodicarboxamide-bridged Triptycenes Molecular Transmission Devices: Converting Rotation to Rocking Vibration

Guangxia Wang,[†, §, ‡] *Lishuang Ma,*[§] *Junfeng Xiang,*[†] *Ying Wang,*[*, §] *Xuebo Chen,*[*, §] *Yanke Che,*[*, †] *and Hua Jiang*[*, †, §]

[†] Beijing National Laboratory for Molecular Sciences, CAS Key Laboratory of Photochemistry, Institute of Chemistry, Chinese Academy of Sciences, Beijing 100190, China

[§] Key Laboratory of Theoretical and Computational Photochemistry, Ministry of Education; Chemistry College, Beijing Normal University, Beijing 100875, China

[‡] University of Chinese Academy of Sciences, Beijing 100049, China

Email: jiangh@bnu.edu.cn, ywang1@bnu.edu.cn, xuebochen@bnu.edu.cn and ykche@iccas.ac.cn

RECEIVED DATE (will be automatically inserted after manuscript is accepted).

TOC Graphics

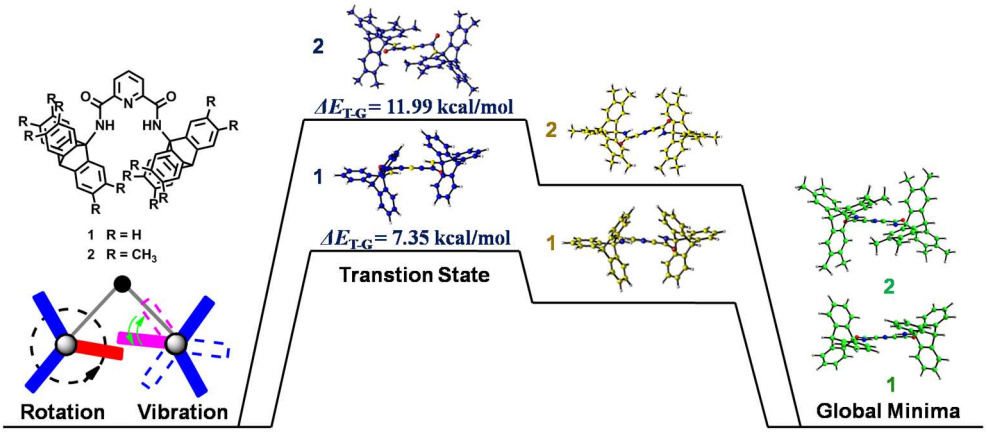

ABSTRACT: A serial of N^2,N^6-bis(triptycene-9-yl)pyridine-2,6-dicarboxamides **1**–**4** were designed and synthesized. Due to rotational constraint of 2,6-diamidopyridine bridge, the triptycene components in the systems are held together. X-ray structures of **1**–**4** show that the molecules adopt a gear-like geometry in the solid states. DFT (B3LYP/6-31G(d)) calculations predict the gear-like C_2 conformation as global minimum structures for **1** and **2**, and suggest that, through a slippage transition process, rotation of one triptycene component would give rise to a rocking vibration of the counter one due to the barrier for rotation of the triptycene components. VT NMR studies on **1**–**4** show that the pair of triptycene components undergo ceaseless slippage at room temperature, but nearly freezes at temperature as low as 183 K. Decreasing the temperature freezes the slippage between triptycene components as well, thus producing the appearance of phase isomers of **3**–**4**. The dynamic features of the studied molecules indicate that this kind of molecules is able to function as a kind of molecular transmission devices for transforming the mode of motion from rotation to rocking vibration.

INTRODUCTION

Artificial molecular machines[1, 2] have attracted considerable interest due to their attractive potential in construction of ultraminiaturized machines. During the past decades, a variety of molecular machines, such as molecular gears[3], molecular shuttles[4], molecular brakes[5], molecular turnstiles[6], molecular motors[7, 8] and molecular gyroscopes[9, 10], have been rationally designed and constructed to mimic their macroscopic counterparts. However, few of them adapts mechanical principles from the macroscopic transmission devices used for transforming the mode of movements, although these kinds of machinery components are indispensable in all macroscopic machines.

On the other hand, as a kind of molecular rotary devices, molecular gears couple two or more submolecular rotatory components in one molecule, so as to rotate correlatively, to mimic the cogwheeling rotation of macroscopic gears. The three-bladed 9-triptycene (Tp) is well known as an excellent moiety to build up molecular gears due to its rigid and shape-persistent structure.[1] Since the pioneering studies of Mislow and Iwamura,[11-16] a variety of molecular bevel gear systems based on derivatives of Tp have been designed and synthesized, in which the intermeshed Tp components are coupled by various static atoms or groups, such as CH_2[11, 13, 15], O[12, 13, 15], S[15], CHOH[15], CO[13a], SiH_2[15], NH[14, 15], HC=CH[17], GeCl[16c, 16d] and SiF_2[18] (Figure 1). Due to the small axle–axle distance between Tp groups, these molecular bevel gears (Tp_2X or Tp_3X) possess a low energy barrier (1~2 kcal mol^{-1}) for disrotatory cogwheeling (geared rotation) but exhibit a comparatively much higher barrier (> 30 kcal mol^{-1}) for correlated conrotations (take place in the process of gear slippage),[11a] indicating that these tightly meshed gears undergo unhindered rotational motions with high gearing fidelity[19]. Accordingly, the ground and the transition states (with C_2 and C_s conformation, Figure S1) presenting in geared rotation are almost isoenergetic, while the gear-clashed conformation (C_{2v}) has a much higher energy.[11a]

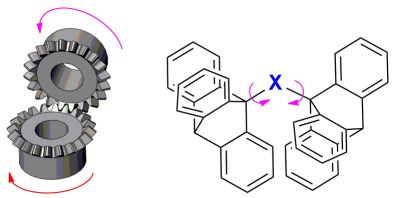

Figure 1. Macroscopic bevel gear and a model for the structure of the reported molecular bevel gears Tp_2X (X = O, CH_2, S, CHOH, CO, SiH_2, NH, HC=CH or SiF_2. The groups C_3H_2 and GeCl are also used to assemble a cyclic gear with the structure which can be expressed as Tp_3X).

The energy gap between gear-clashed conformation and the ground state, which can be estimated from the activation energy for gear-slippage process, highly depends on the distance between Tp groups. Longer interaxle distance would typically give rise to a lower barrier. For example, the activation energy for slippage was measured to be 42~43 kcal mol^{-1} in chloro-substituted Tp_2O[12c] (with C(9)–O bond length ($d_{C^9–O}$) of 1.41~1.42 Å and C(9)–O–C(9') bond angle ($\varphi_{C^9–O–C^{9'}}$) of 136°), 32~33 kcal mol^{-1} in that of Tp_2CH_2[13c] (with $d_{C^9–C}$ of 1.53~1.57 Å and $\varphi_{C^9–C–C^{9'}}$ of 129°) and ~21 kcal mol^{-1} in Tp_2SiH_2[15] (with $d_{C^9–Si}$ of 1.86 Å and $\varphi_{C^9–Si–C^{9'}}$ of 129°). Along this line, one may be curious how the dynamic properties of such molecular gears change when the interaxle distance increases further. It has been demonstrated (and is also easy to image) that gearing would lose the efficiency completely when the gears are declutched.[18] But what if the distance keeps increasing but still within a point where the two rotators remain interaction? And, is that possible to develop a new molecular devices derived from the bevel gears at this state?

To visualize the dynamic properties of such loosely-coupled molecular bevel gears are challenging, considering the uncertainty and diversity in the steric repulsion between Tp groups and the interaxle distance in those unknown systems. A little trick is treating the systems as spur gears first, with a presupposition that the Tp rotators are connected with a spring-like tension. In this model, given the rigid structure of rotators, the length of spring under its equilibrium position is very important. A short spring with the length close to that of the radii of Tp rotators would provide a tightly meshed molecular gear, like most of the reported ones[11-18], with ceaseless dynamic interconvertion between C_2 and C_s states (Figure S1). The C_2 conformation is stabilized by π stacking and orbital interactions, whereas the C_s one by orbital interactions only. With the increase of the length of spring, the orbital interactions are

expected to weaken gradually. To a point, the C_s conformation might not be a local energy minimum any more. In this process, the gearing fidelity[19] would decrease, which means C_{2v} (represents gear slippage) and C_{2v}^* conformations[20] might be two important transition states in the process of gearing (Figure S1). The maximum axle–axle distance for C_{2v}^* orientation is larger than that of the C_{2v} one. Consequently, if the interaxle distance is between the two maximum axle–axle distance for C_{2v} and C_{2v}^* orientations, there should be no interaction between two rotators when the gear adopts C_{2v} conformation, which means that there would be a break in the process of rotation transmission from one rotator to the counter one. This is interesting because if the counter rotator could rotate back in every single break with certainty, the rotation of the driving rotator would give rise to a vibration of the counter one. Consequently, the system would not be a molecular gear with low gearing fidelity any more, but a device which could be used to transform the mode of motion. Nevertheless, these speculations are only based on a very simplified mechanical model. Without a concrete molecular model, what on earth are the transitional states as well as the changes of energy gaps between different states under such conditions compared to that in tightly meshed mode are hard to predict, and those will be more complicated when the model is propagated to real molecule under different conditions.

To date, no molecular bevel gears with large interaxle distance are reported. Bryan has previously reported that the incorporation of Tp units into crown ether created a spur-gear-like structure, but the rotators in it are too far from each other to intermesh.[21] Recently, molecular spur gears with Tp groups bridged with bibenzimidazole were rationally designed and described by Siegel.[20] However, in despite of considerable energy barriers for gear slippage (calculated to be ~8 kcal mol^{-1}), the interconversion between phase (*dl* and *meso*) isomers[11a] could not be experimentally observed.

In this contribution, we describe the design, synthesis, X-ray structure and the dynamic properities of 2,6-pyridinedicarboxamides-bridged Tp derivatives **1**–**4**, which are derived from the conventional molecular gears. Due to the appropriate length of the static bridge as well as the large rotation barrier of Tp components, these molecules behave as a kind of molecular transmission devices for transforming the mode of motion from rotation of one Tp component to rocking vibration of the counter one. To theoretically figure out the most energetically favourable conformational transformation path in the process of intramolecular movement transmission, the minimum energy profiles (MEPs) as a function of the dihedral angle between the planes of one benzene ring in a rotator and the adjacent amide were calculated for **1** and **2** using density functional theory (DFT). Besides, dynamic ^{1}H and ^{13}C NMR measurements were also carried out to study the dynamic features of **1**–**4** in solutions.

RESULTS AND DISCUSSION

Molecular Design. A molecule that suitable for studying the rotation of the molecular bevel gear should at least: (i) be structurally rigid and shape-persistent under gearing; (ii) have static group with suitable length thus keeping the two rotators at an appropriate distance; (iii) maintain the two rotation axles of rotators coplanar while rotating and (iv) allow for experimental observation of the intramolecular motions.

Previous studies[22] have shown that 2,6-pyridinedicarboxamides prefer to adopt a stable, *cis*-conformation ascribed to the intramolecular hydrogen-bonding between amide and pyridine-N, providing a good motif to construct bent supramolecules such as foldamers. Meanwhile, due to the sp^2 hybridization of the nitrogen atom in amides, the entire 2,6-pyridinedicarbox amides group is planar, which renders the two rotators rotating around two separate axles within the same plane if this moiety is

used as the static in the molecular gears. Furthermore, in contrast to the small axle–axle distance in the molecular bevel gears those reported previously[11-18], the distance between two amido nitrogen ($d_{N\cdots N}$) in 2,6-pyridinedicarboxamide group is as large as ca. 4.6 Å according to the molecular structure, which is about 3.5 fold longer than that of typical double bonds ($d_{C=C}$ = 1.3 Å in ethylene) and about twice as the width of a benzene ring (2.4 Å)[23]. All these concepts inspired us to design molecules **1**–**2** based on 2,6-pyridinedicarboxamides-bridged Tps, in which the methyl substituents on **2** were designed to increase the size of gear blade thus being useful for studying the effect of the blade size of rotators on the dynamic properties.

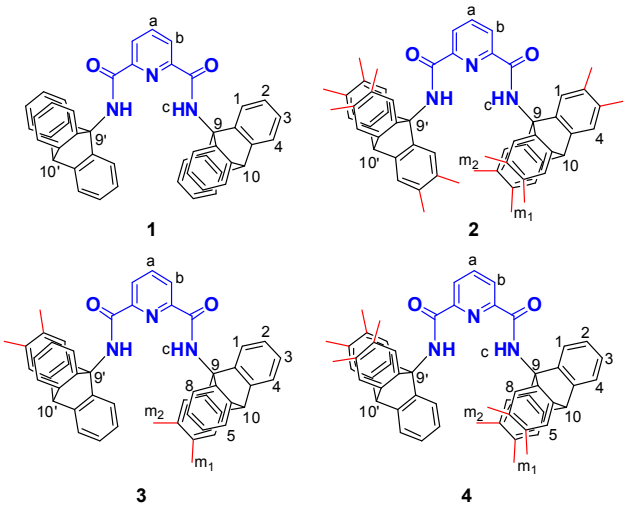

In the conventional Tp-based molecular gears, the subsitituents on the bridgehead carbons were typically designed to produce negligible steric interference with the rotary of rotators.[20, 24] By this way, the effect of stereodynamics of subsitituents themselves on that of gearing could be ignored. This method could simplify the stereochemistry analysis of the gearing behaviors, but will give rise to rapid and frictionless rotation of the Tp groups (no matter with or without cogwheel rotation) which are not detectable on the NMR time scale. For the designed molecules, the introduction of amide would destroy

the symmetry of the Tp group and produce an extra rotation energy barrier arising from the steric effect of carbonyl oxygen atom of the amide, in which the extra rotational barrier might increase the coalescence temperature in dynamic NMR experiments thus rendering the rotation of Tp to be technically measurable. More importantly, this extra barrier might be able to define an equilibrium position of the Tp components, by which the Tp groups keep a trend to rotate back as long as it deviates from the equilibrium position.

Molecules **3**–**4**, which have two and four methyl subsitituents on each Tp rotators, respectively, and could be regarded as a hybrid of **1** and **2**, were designed for better understanding the relationship between the size of rotators and the dynamics for the studied systems. Besides, it is noteworthy that, different from molecules **1** and **2**, the subsititution of methyl groups on **3**–**4** will break the equivalence of three benzene rings on each Tp groups, giving rise to phase isomers.

Synthesis. Synthetic routes for molecular bevel gears **1**–**4** are outlined in Scheme 1. The key issue in these approaches is to obtain the 9-triptycylamine derivatives, that is, the methyl-substituted 9-triptycylamines.

Tp derivatives are generally synthesized by the Diels-Alder reaction from the corresponding anthracenes and benzynes.[25] However, as pointed out by Yamamoto,[26] this method is unfeasible for 9-triptycylamine derivatives because of the presence of undesirable hydroamination of the amine group with benzynes. The preparation was thus initiated with the 9-nitroanthracene or its derivatives. Addition of excess of benzenediazonium-2-carboxylate in portions to the solution of 9-nitroanthracene while refluxing provides benzyne in situ by thermal decomposition, which then undergo Diels-Alder reaction to give the 9,10-adduct, 9-nitrotriptycene (**10**), in 46% yield. The low yield is ascribed to the strong

Scheme 1. Synthesis of 2,6-Pyridinedicarbox amides-bridged Triptycene and its Derivatives **1**–**4**[a].

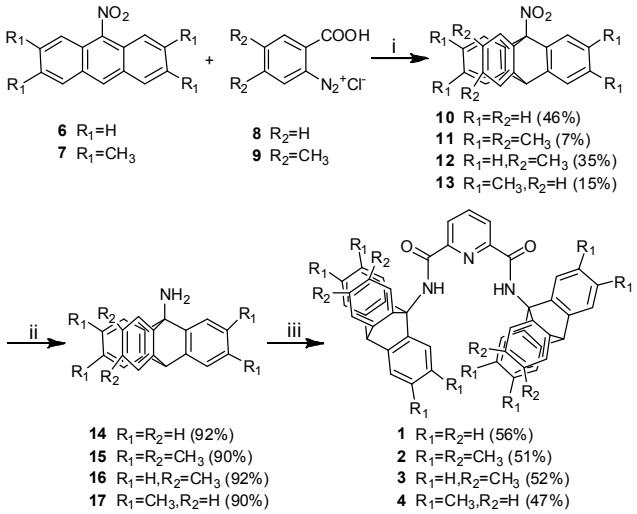

[a] Reagents and conditions: [a] Reagents and conditions: (i) 1,2-epoxypropane, CH_2ClCH_2Cl, reflux; (ii) $SnCl_2$, HCl, CH_3COOH, reflux; (iii) 2,6-Pyridinedicarboxylic dichloride, DIEA, CH_2Cl_2, rt (for **1**, **3** and **4**); or 2,6-pyridinedicarboxylic acid, PyBOP, DMAP, DMF, reflux (for **2**).

electron withdrawing of nitro group, which is not favorable for the Diels-Alder addition thus giving considerable amount of 1,4-adduct, 11-nitro-5,12-dihydro-5,12-ethenonaphthacene. The multiple methyl group substituted 9-nitrotriptycenes were prepared from the corresponding derivatives of 9-nitroanthracene and benzenediazonium-2-carboxylate. For example, while 2,3,6,7,14,15-hexamethyl-9-nitrotriptycene (**11**) could be prepared from 2,3,6,7-tetramethyl-9-nitroanthracene (**7**) and 4,5-dimethyl-benzenediazonium-2-carboxylate (**9**), reaction of **7** with 4,5-dimethyl-benzenediazonium-2-carboxylate (**8**) gave 2,3,6,7-tetramethyl-9-nitrotriptycene (**13**). It was found methyl substitution is to the disadvantage of producing desirable 9,10-adducts, which is probably due to the increased steric hindrance of the methyl group. Careful isolation of the additive productions gave **11** in only 7% yield,

but a bit higher for **12** and **13** as 35% and 15%, respectively. Reduction[27] of **10**–**13** with $SnCl_2$ in the acidic condition provided the corresponding aminotriptycenes **14**–**17**. Amidation of **14** with 2,6-pyridinedicarboxylic acid chloride, using *N*,*N*-diisopropylethylamine (DIEA) as the base, gave the target compound **1** with the yield of 56%. However, the analogous convergent method to compound **2** was not successful, in which the reaction was found to be hard to proceed even under refluxing in toluene. Fortunately, **2** can be obtained in acceptable yield by coupling of **15** and 2,6-pyridinedicarboxylic acid with the help of peptide coupling reagent benzotriazol-1-yl-oxytripyrrolidinophosphonium hexafluorophosphate (PyBOP). The final two target compounds **3** and **4** were prepared according to the method described for **1**. Structures of **1**–**4** are confirmed by NMR and high resolution mass spectra. The assignments of their experimental ^{1}H and ^{13}C NMR spectra were performed based on the corresponding ^{1}H–^{13}C HSQC, ^{1}H–^{13}C HMBC, ^{1}H–^{1}H NOESY and ^{1}H–^{1}H COSY experiments (see Figure S2–S11 in the Supporting Information (SI)).

X-ray structures of 1 and 2. Crystal structure of **1** was obtained by slowly evaporating the solvent of mixture of dichloromethane (DCM) and methanol at ambient temperature (Figure 2a). The crystal is an orthorhombic, solvent-contained system, with space group of P2(1)2(1)2(1). Each unit cell contains four molecules of **1** and four of DCM, packed with high disorder. As expected, in the structure, the central bridge 2,6-pyridinedicarboxamido group adopted a preferred *cis* conformation ascribed to the hydrogen bonding between pyridine-N and amido-NH (the N−H···N(pyridine) distance of 2.43 and 2.22 Å), holding the two Tp groups together to assemble a molecular bevel gear-like structure in C_2 conformation. The structure is not entirely symmetrical. While one amido group maintains a planar geometry with the core pyridyl group, the other is slightly twisted (with dihedral angles of 6°) to accommodate the sterics.

Meanwhile, despite there is one blade (one phenyl ring) directed *endo* in both rotators, the inward-facing ring in one rotator is more planar to the plane of pyridine (intersecting at an angle of 16°), but the counter one on the other Tp group is significantly more torsional (dihedral angles of 59°). The distances between the (9−9′) and (10−10′) bridgehead atoms of the Tp groups are 6.64 and 10.16 Å, respectively, providing the distance between two center of the Tp axles of about 8.4 Å, which is larger than the minimum axle−axle distances (7.0 Å) calculated by Siegel for a Tp-based molecular spur gear in C_2 conformation.[20] Notably, although by wireframe representation two rotators seem separated apart, a space-filling mode (Figure 2a, right) reveals that they in fact partially stack with each other, suggesting they are able to behave correlated motion at least when **1** adopts ground state conformation.

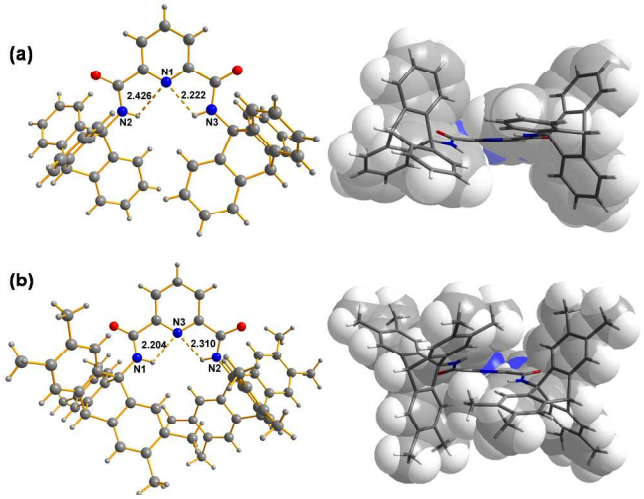

Figure 2. The ball and stick diagrams (Left, top view) as well as the stick diagrams overlaid by Diamond 3.0 generated space-filling representation (Right, side view) for molecular structure of (a) **1** and (b) **2** which crystallized from the mixture of dichloromethane and methanol. The contained dichloromethane molecules in the cell unit of **1** were omitted for clarity.

Single crystal of **2** can also be obtained from the solution in the mixture of dichloromethane and methanol (Figure 2b). The crystal is a monoclinic, with space group of P2(1)/n. Each unit cell contains only four molecules of **2**. Similar to that of **1**, the intramolecular hydrogen bonding constrains the methyl-subsitituted Tp groups, providing a gear-like structure in C_2 conformation, wherein the two amides are twisted and tilted up and down along the plane of pyridyl group with the dihedral angles of 17° and 19°. The diminish in planarity compared to that of **1** is ascribed to the bigger steric exclusion from two methyl-subsitituted Tp groups when compared to that of unsubsitituted ones. The distances between the (9−9′) and (10−10′) bridgehead atoms of the Tp groups are 6.40 and 9.72 Å, which are a bit smaller than those in the structure of **1**. This probably dues to the stronger π stacking and orbital interactions between two Tp groups of **2**, as suggested by the fact that the distance between the planes of two proximal benzene rings on one Tp group and the closest methyl protons on the counter Tp one are just about 3.05 Å. A space-filling mode (Figure 2b, right) clearly shows that the two Tp groups intermesh more tightly in comparison with that of **1**, providing hope of possessing a higher efficiency of motion transmission.

Calculations. While some of the prevoius computational studies on molecular bear or spur gears directly focus on the molecular geometries and the relative energies of C_2, C_s and C_{2v} conformations,[11-14, 20] identification of the motion profile as well as the ground and the transition states within it for the studied system needs to determine the most energetically favourable conformational transformation pathway, i.e., MEP, considering the motions in the studied systems might be considerably different from those of the molecular gears. Therefore, starting from the X-ray structures, the unconstrained geometries of **1–2** were first optimized and confirmed to the global minima at DFT level of theory with the B3LYP

hybrid functional and the 6-31G* basis set. Then, from this point, the MEPs were obtained by relaxed potential energy surface scan procedures[28, 29] implemented in the GAUSSIAN 03 program package[30] as a function of the dihedral angle (denotes ϕ) of C_{17}(carbonyl)–N_{14}(amide)–C_{51}(bridgehead)–C_{70}(ring α) for **1** and C_{17}(carbonyl)–N_{14}(amide)–C_{47}(bridgehead)–C_{71}(ring α) for **2** (could be approximately regarded as the dihedral angle between the planes of benzene ring α and the adjacent carbonyl group) (Figure S17). At each point on the MEPs, all the degrees of freedom other than the fixed dihedral angle were allowed to be fully optimized. Given the three-fold symmetry of Tp group, the dihedral angle was scanned totally by 120° with a step size of 1°. To verify the transition states obtained by scan strategy (scanned TSs), we re-optimized two transition states by using the conventional TS optimization method (to give optimized TSs) along the reaction pathways of the rotational isomerization of **1** and **2**. In this case, all the degrees of freedom are completely relaxed without any predefined reaction coordinates. All computational results were summarized in Figure 3 and Figure 4.

DFT calculation confirms the C_2 conformation as the global minimum for **1** by vibrational analysis (Figure 3). The optimized geometry bears a close resemblance to the X-ray structure (Figure 2a). For example, the distances between the (9−9′) and (10−10′) bridgehead atoms of the Tp groups are predicted to be 6.88 and 10.62 Å, and the central bridged moiety 2,6-pyridinedicarboxamide is also almost planar. The dihedral angles between the planets of two benzene rings directed *endo* (α and α′, Figure 3) and the plane of pyridyl group are measured to be 17.7° and 17.6°, indicative of slightly more symmetrical structure when compared to that in the crystal. The motion of **1** is predicted to start with a gearing.

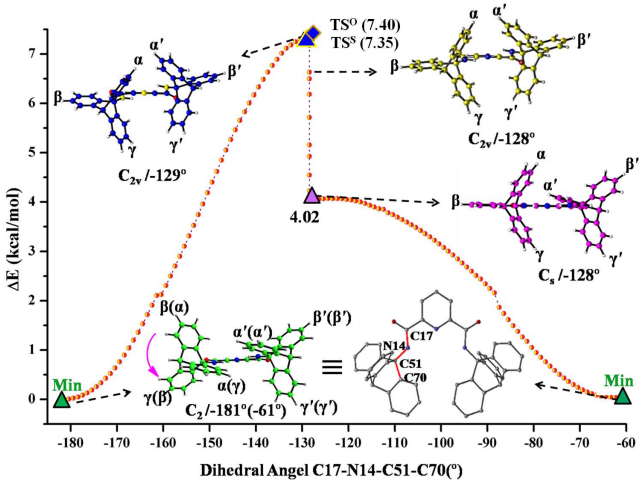

Figure 3. Minimum energy profile of rotational isomerization of **1** along C17-N14-C51-C70 (ϕ) dihedral angle calculated by relaxed potential energy surface scan at the B3LYP/6-31G (d) level of theory. The transition states were calculated by scan strategy (TS^S) and direction method of conventional TS optimization (TS^O), respectively.

Rotating the Tp moiety where benzene ring α located anti-clockwise from ϕ dihedral angle of −181° gives rise to a slight distortion of pyridylamides (Table S2, SI) and, more importantly, a disrotation of the counter Tp group, accompanying by a considerable increase in energy ascribed to the steric hindrance of carbonyl oxygen. The highest energy comformer of the energy curve, which shows up at the point where ϕ dihedral angle is −129° and is ca. 7.4 kcal mol^{-1} higher in energy than that in the minimum conformation, adopts an approximately gear-clashed C_{2v} orientation, suggesting that the gearing will lose fidelity soon. Notably, a temporary C=O···H−C hydrogen bond between the carbonyl oxgen and the proton H_{38} on benzene ring β is predicted to be present in process of that ring β passes over the carboxyl group, and the strongest bonding (with H···O distance of 1.98 Å and H−C···O bond angle of 114.5°) occurs when these two groups are nearly coplanar, wherein ϕ = −129°. This hydrogen-

bonding might be able to stabilize the C_{2v} transition state, thus, to some extent, lowering the rotational barrier of the Tp group.[31] Besides, the scanned TS shows negligible differences in geometric structure (deviation: 0.02-1.26°/dihedral angles; 0.0-0.002Å/bond lengths) and relative energy (deviation: 0.05 kcal mol^{-1}) compared with the one obtained by the direct method of the conventional TS optimizations (see Figure 3 and Table S4 in SI). Frequency calculation on this scanned TS yields one and only one imaginary frequency (41.67i cm^{-1}) corresponding to the rotational motion of triptycene along the axle of C(triptycene)–N(amide) bond, which is very closed to the optimized TS (41.75i cm^{-1}) with the same vibration mode. Intrinsic reaction coordinate (IRC) calculations starting from optimized or scanned TSs confirm that these energy maxima unambiguously connect with the corresponding reactant of ground state minima along the reaction paths of triptycene rotation along the axles of C-N bond. These suggest that there are no principal differences in describing the rotational isomerization of triptycene by using the scan strategy and the direct method of transition state optimization, and also indicate that it is reasonable to choose C17-N14-C51-C70 dihedral angle as the reaction coordinate in the MEP calculations of this rotational isomerization. As expected, with just a slightly continuous rotation of the driving Tp group from −129° to −128°, the gear slips and the counter Tp group rotates back (anti-clockwise), accompaning with a drastic reduction (3.3 kcal mol^{-1}) in energy. The reverse rotation is ascribed to the relatively too large interaxle distance as well as the rotation barrier for the counter Tp rotator. Another important transition geometry, which adopts an approximate C_s conformation, is observed at ϕ = −128°, in which the dihedral angle between the planes of ring α′ and pyridyl group is 13°, pretty close to that in the minimum conformation. With further rotation of the driving Tp rotator to the final where ϕ = −61°, the counter Tp moiety keeps almost stable, while the energy moderately

decreases. These computational results clearly show that rotation of one Tp rotator on **1** would give rise to a vibration of the counter one, indicating that rotation-drived vibration is the main mode of the intramolecular motion of **1** as we designed.

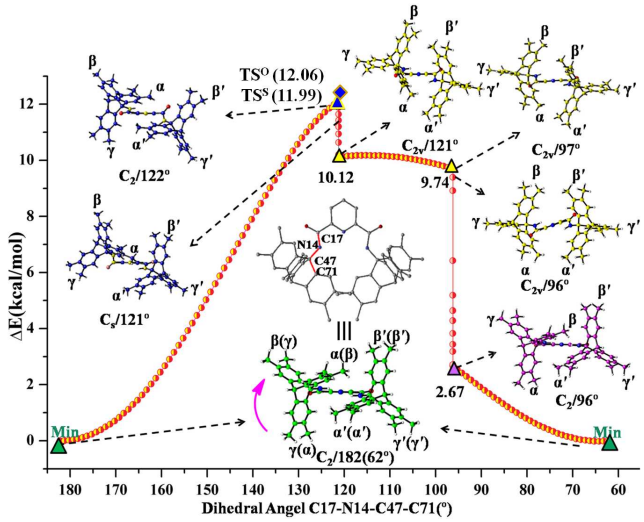

Figure 4. Minimum energy profile of rotational isomerization of **2** along C17-N14-C47-C71(*ϕ)* dihedral angle calculated by relaxed potential energy surface scan at the B3LYP/6-31G (d) level of theory. The transition states were calculated by scan strategy (TS^{s}) and direction method of conventional TS optimization (TS^{o}), respectively.

In contrast to **1**, the DFT calculation on molecule **2** predicts a slightly more complicated intramolecular movement profile (Figure 4). The global minimum of **2** possesses a C_2 conformation and closely resembles its single crystal geometry (Figure 2b), wherein the central 2,6-pyridine dicarboxamide moiety is planar and the dihedral angles between this moiety and both the plane of benzene ring α and α′ are 23°. At this state, the *ϕ* dihedral angle was measured to be 182°. Different from that of **1**, clockwise rotation of the Tp group where benzene ring α is located initailly gives a

distortion of the adjacent amide and a gradual increase in energy, but does not induce perceptible anti-clockwise rotation of the counter Tp group. This is probably ascribed to the big methyl-substituted Tp rotators, which is larger in the radius than the minimum axle-axle distance required for the C_s orientation so that the pyridylamide connected to the driving rotator should at first deform to accommodate the crescent sterics. The highest energy comformer, which lies ca. 12.0 kcal mol^{-1} higher in the energy level than that of the global minium, shows up at ϕ = 122°, where the pyridylamide connected with the driving rotator is seriously distorted while the counter Tp-amide is almost still under the equilibrium position. Similar to the case of **1**, the highest energy conformer obtained by scan strategy (i.e., TSs) is very close to the one computed by conventional TS optimizations along the unbiased reaction coordination of **2** (Table S5). This reveals that the rotational isomerization proceeds along the axle of C(triptycene)–N(amide) bond is the predefined reaction coordinate in our scan strategy. Continuous rotation of the driving rotator leads to an apparent disrotatory motion of the counter Tp group, through a way of the anti-clockwise rotation of the counter Tp group around C_{23}(Tp)–N(amide) bonds as well as the deformation of the pyridylamide connected (Table S3, SI). The strain in the whole molecule thus gets released, giving a sharp decrease in the energy. Surprisingly, in the range of ϕ = 121°−97°, rotation of the driving rotator once again produces only the deformation of the connected amide, which gives rise to a transient increase in the interaxle distance and a slight decrease in energy. Subsequently, through a gear-clashing transition (C_{2v}/96°, Figure 4), the position of benzene ring α and α′ reverses, providing a new transition structure in which the counter Tp almost returns back to its equilibrium position. This is distinctly different from what we hypothesized, as we expected that the methyl substituents would increase the size of rotator's blade thus benefiting gearing. Obviously, the

rotation barrier of Tp group was underestimated in our design. In fact, this barrier is so high that the molecule prefers to weaken the N−H···N (pyridine) hydrogen-bonding and distorting the amide group to behave slippage rather than overcoming an additional rotation barrier from the counter rotator. Further rotation of the driving Tp group from ϕ = 96° releases the strain arising from the torsion of pyridylamides, providing a moderate decrease in energy until finally a global minimum geometry is re-obtained. All these predict that the methyl substituents would not change the basic mode of motion of **1** but will increase the energy barrier of slippage thus raising the free energy of activation for the overall motion transmission.

VT-NMR experiments of 1 and 2. Experimentally studies on the motions of **1** and **2** in solution were carried out with NMR spectroscopy rather than other methods, such as time-resolved emission spectroscopy[32] (internal rotation in the studied molecules would be too slow on the timescale of fluorescence emission, giving the fluorescence lifetimes are generally on the order of 1-10 nsec). At ambient temperature, the Tp groups rotate fast around C_9 (Tp)–N(amide) bonds on the NMR time scale, giving the six benzyl rings on Tp moieties magnetically equivalent. Consequently, the ^{1}H NMR spectrum of **1** in CD_2Cl_2 at 298 K shows only one set of sharp signals of benzyl rings (i.e., two doublets at 7.48 and 7.54 ppm those are assigned to protons H_1 and H_4 as well as two triplets at 7.02 and 7.12 ppm for H_2 and H_3, respectively). In addition, the amide protons exhibit one single signal at 9.61 ppm as well. In the corresponding ^{1}H−^{1}H NOESY spectrum (Figure S2), the cross-peaks between amide protons and their neighboring pyridinyl protons are completely absent, demonstrating that the central bridge 2,6-pyridinedicarboxamides unit is mainly rotationally constrained in solution as that in the solid structure.

To explore more dynamic features of **1** in CD_2Cl_2, variable-temperature (VT) ^1H NMR investigations were then carried out (Figure 5a and Figure S18). While the pyridyl protons signals of **1** show no changes at all upon the decrease of the temperature in the range examined (Figure S18), the Tp protons, especially the protons H_1 and H_2 close to counter Tp rotator, undergoes slight upfield and downfield shift, respectively, at the beginning of this process. The changes in the chemical shift are ascribed to the increase in the fraction of **1** in the ground state conformation. Decreasing the temperature further provides considerable broadening of H_1 and H_2, clearly indicating that the Tp-N rotations slow down upon lowing the temperature. The decoalescence of H_1 and H_2 were observed at 203 K. This comparatively high coalescence temperature in comparison with all those tightly meshed molecular gears[12a] is due to the steric hindrance of carbonyl oxygen atom as well as the slippage process, arising

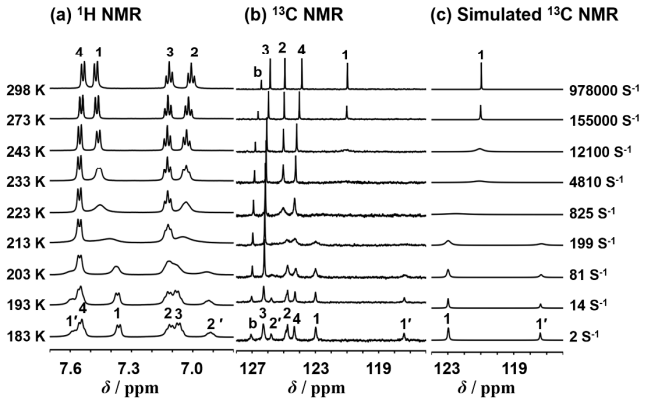

Figure 5. a) Partial VT ^1H NMR spectra (500 MHz) of **1** (2 mM) in CD_2Cl_2. b) Partial VT ^{13}C NMR spectra (125 MHz) of **1** (40 mM) in CD_2Cl_2. c) Simulated VT ^{13}C NMR spectra at the region of carbon C_1, which were obtained with DNMR Line shape Analysis procedure implemented in the Topspin 2.1 program[33]. The temperature (K) and calculated interconversion rate constants (k_r, s^{-1}) are given for each trace.

energy barrier to Tp-N rotations. With even further decrease in the temperature, the rotation of Tp groups becomes frozen and thus either of the H_1 and H_2 signals split into two peaks, with an intensity ratio of 2:1. The ^{1}H NMR spectra in this case mainly correspond to **1** in ground state conformation, where the protons H_1 and H_2 show small peaks at 7.58 and 6.91 ppm, respectively, which can be assigned to the relevant protons on the inward-facing benzene rings (labelled as α and α′ in Figure 3), and larger peaks at 7.36 and 7.11 ppm, respectively, to the corresponding protons on the other four rings. The smaller peak of H_2 signal is upfield from the bigger one, which is ascribed to ring-current effects arising from π-stacking interaction between rings α and α′. In contrast, the signals of H_1 on ring α and α′ locates downfield which is probably ascribed to the deshielding of pyridine-N (3.57 Å for the distance of C_1−N(pyridyl) in the crystal structure). Expectedly, the benzene rings β and γ are not chemically equivalent in case of **1** in ground state as predicted by DFT calculation (Figure 3), as evidenced by that the signals of H_1 at 7.36 ppm and H_2 at 7.11 ppm split further when the temperature is as low as 183 K. It is noteworthy that, in the whole process, the chemical shift of amide proton remains almost unchanged ($\Delta\delta$ = 0.07 ppm) (Figure S18), which indicates that, throughout the entire range of temperature examined, the intramolecular H-bonding between pyridine-N and amide always presents and that the N−H···N (pyridine) bonding pattern (including the bond angle and bond distance) does not change much upon the change of temperature. This is important because it experimentally once again demonstrate that, the molecule keeps adopting a gear-like conformation in the motion, as previously indicated by the ^{1}H−^{1}H NOESY spectrum.

The mulitiplicity and overlap of some important protons signals of **1** prevents a direct line-shape analysis of the ^{1}H NMR spectra for elucidating the kinetic parameters for the motions of **1**. To

circumvent this problem, VT ^{13}C NMR experiment was carried out (Figure 5b and Figure S19).[34] Similar to that of VT ^{1}H NMR experiment, upon lowing the temperature, the signals of C_1 and C_2 gradually broaden and decoalesce at about 213 K. At 183 K, two pair of sharp peaks with a 2:1 ratio in intensity for C_1 and C_2 were observed. The rate constant corresponding to the process that any one of the benzene rings passes over the carbonyl group were derived from the line shape analyses of the C_1 resonances (Figure 5c). From these constants, the free energy of activation ($\Delta G^{\#}$) as well as the enthalpy ($\Delta H^{\#}$) and entropy ($\Delta S^{\#}$) were derived from the Eyring plots[35] (Table 1, Figure S20), in which $\Delta G^{\#}$ is calculated to be 9.0 kcal mol^{-1} that is pretty close to DFT-calculated energy gap between the transition state (TS^s and TS^o) and the minimum conformers.

Table 1. The Summary of the thermodynamic Parameters for **1**–**4**.

Compd.	N_{methyl} [a]	$\Delta G^{\#}_{298\ K}$ (kcal mol^{-1})	$\Delta H^{\#}$ (kcal mol^{-1})	$\Delta S^{\#}$ (cal mol^{-1} K^{-1})
1 [b]	0	9.0 ± 1.0	12.3 ± 0.4	11.0 ± 2.0
2 [c]	12	11.0 ± 0.2	9.2 ± 0.1	-5.9 ± 0.4
2 [b]	12	11.0 ± 0.2	9.2 ± 0.1	-5.9 ± 0.3
3 [b]	4	9.0 ± 0.7	12.3 ± 0.3	11.0 ± 1.2
4 [c]	8	10.8 ± 0.4	8.9 ± 0.2	-6.3 ± 0.7

[a] Number of methyl substituents on the molecule. [b] These values were obtained from VT ^{13}C NMR experiments. [c] These values were obtained from VT ^{1}H NMR experiments.

We next performed VT ^{1}H and ^{13}C NMR experiments on **2** in CD_2Cl_2 (Figure 6, Figure S21, S23 and S24). Similar to that of **1**, Decreasing the temperature slows down and finally freezes the rotation of methyl-substituted Tp groups, giving rise to broadening followed by splitting of the signals of the protons and carbons which are spatially close to the counter Tp group. In this process, the chemical shift

of amido-NH just slightly downshifts ($\Delta\delta$ = 0.15 ppm) (Figure S21), which suggests that, similar to that of **1**, the amides are H-bonded with pyridine-N all the time but might be a slightly more distorted at ambient temperature compared to that of **1** statistically. A decoalescence is observed at ca. 213 K for both proton H_1 and carbon C_1, wherein the signals split into two peaks with a 2:1 ratio in intensity. Another decoalescence is found to be around 193 K and 183 K for H_1 and C_1, respectively, in which the resonances split further and exhibit three distinguishable peaks as expected. Line-shape analysis of the VT ^{1}H NMR spectra provides the rate constant of the rotation (Figure 6), which shows that, while the rotation of **2** is as frozen as that of **1** at 183 K, increasing the temperature gives rise to an increase (but less dramatic than that of **1**) in the rotational speed. All these observations indicate that the rotational barrier of the substituted-Tp groups in **2** is a bit higher than that of Tp groups in **1**. Two sets of corresponding thermodynamic parameters were thus derived independently from the VT ^{1}H and ^{13}C NMR spectra (Figure S22 and S26). Both approaches provide very consistent results of 11.0 kcal mol^{-1} (Table 1)[36], which is again consistent with that of the DFT-calculated results (TS^s and TS^o).

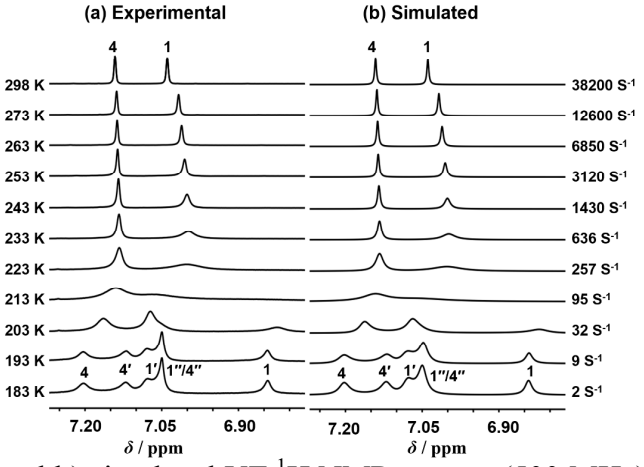

Figure 6. a) Experimental and b) simulated VT ^{1}H NMR spectra (500 MHz) of **2** (2 mM) at the region of H_1 and H_4 in CD_2Cl_2. The temperature (K) and calculated interconversion rate constants (k_r, s^{-1}) are given for each trace.

The fact that $\Delta G^{\#}$ for the rotation in molecule **2** is just a slight larger than that in the case of **1** suggests that both the molecules do not tend to gear, but motions in a way as predicted by DFT calculation. This is because the methyl substituent would not affect the rotation of the whole Tp rotator around C_9(Tp)–N(amide) bonds but only the interaction between two Tp groups while motioning. Consequently, if both the molecules keep gearing, their free energy of activation would be very close, giving the gearing itself is almost unhindered. Besides, it is not likely that **2** keeps gearing while **1** undergoes continuous slippage, since in such case, the molecule **2** needs to overcome the rotation barrier for one more Tp rotators, which would give rise to considerable increase in the free energy of activation when compared to that of **1**. In both cases, $\Delta H^{\#}$ is predominant over $\Delta S^{\#}$ in its contribution to $\Delta G^{\#}$, indicating the rotation is mainly enthalpically disfavorable. The negative value of $\Delta S^{\#}$ in case of **2** suggests that molecule **2** in the transition states have totally less degree of freedom when compared to that in the ground state, probably in such cases, the vibration of some subunits are partially restricted by the torsional strains.

X-ray structures and dynamic behavior of 3 and 4. The crystal structure of **3** was obtained by slowly evaporating the solvent of acetonitrile at ambient temperature (Figure S12a). The crystal is a monoclinic system, and there are four molecules of **3** and four of acetonitrile in each unit cell. The geometry is highly symmetrical, with the two benzene rings with methyl substituent locates flank. The distances between the (9−9′) and (10−10′) bridgehead atoms of the Tp groups are 7.05 and 11.24 Å, respectively, indicating the two Tp groups possess a larger axle−axle distance compared to that of **1** crystalized from the solution of the mixture of DCM and methanol. This larger axle−axle distance is probably induced by cocrystallized acetonitrile molecules in the crystal package, as we later found that crystal structure of **1** with acetonitrile cocrystallized can also be successfully obtained from solution of

acetonitrile and the structure possess larger axle−axle distance than that of the one grown in mixture of DCM and methanol (Figure S12c). The larger interaxle distance is favorable for releasing the steric repulsion between Tp groups, which leads to an approximate C_{2v} conformation in geometry of **3** wherein the dihedral angles between the planes of two benzene rings directed *endo* and the plane of pyridyl group are as small as 2° and 7°, respectively.

Crystals of **4** grown in the mixture of DCM and methanol shows also a symmetrical structure, in which the two benzene rings without methyl substituents directly flank unexpectedly (Figure S12b). There are two molecules of **4** and four of methanol in each unit cell. Nevertheless, the distances between the (9−9′) and (10−10′) bridgehead atoms of the Tp groups are as short as 6.25 and 9.46 Å, respectively, indicative of a slightly more compact conformation than those in the other studied crystal structures.

Since the X-ray structures of **3** and **4** skeletally resemble closely those of **1** and **2** (Figure S13 and S14), we then carried out dynamic NMR studies for better understanding of the dynamic properties of this type of molecules. Due to the fast rotation of Tp groups at ambient temperature, the ^{1}H NMR spectrum of **3** in CD_2Cl_2 at 298 K shows only one set of sharp signals of the amides and the benzene rings without methyl substituents (Figure S27). Decreasing the temperature below 233 K gives rise to broadening of all Tp signals and splitting of the signals of unsubstituted benzene rings, wherein the decoalescences of H_1 and H_2 occur at ca. 203 K. Notably, in this process, decoalescences of amide-NH and pyridonyl protons were observed at 193 K, which is ascribed to the appearance of phase isomers (Figure S35 and S36). The splitting of Tp signals arising from the presence of phase isomers is hard to distinguish due to the overlap of signals. Integration analysis shows two phase isomers exit in ca. 2:1 ratio, consistent with the observation for most molecular gear systems[11b, 18]. Similar phenomena could

be also observed on the corresponding VT ^{13}C NMR spectra, wherein decoalescences of several Tp carbons such as C_1 and C_2 are observed at ca. 213 K and the phase isomers starts to show up at ca. 203 K (Figure S28 and S29). Clearly, in both the VT ^{1}H and ^{13}C NMR experiments, the signals of Tp groups decoalesce at a bit higher temperature when compared to that of the appearance of the phase isomers. This is understandable. Since that given the energy barrier for vibration is much lower than that for rotation, even under certain conditions the rotation of Tp rotators is freezing, it is still possible for the vibration to take place, providing possibility of slippage thus inhibiting the appearance of phase isomers. Consequently, for the studied cases, decoalescence of Tp signals might not always synchronize with that of amides, especially for system which possess rotators with short blades such as **3**. On the other hand, the fact that the phase isomers could not be observed above 203 K indicates the two Tp rotators keep slipping in those cases, providing evidence of that the rotation of the driving rotator gives a vibration of the counter one. Calculation of the thermodynamic parameters for Tp rotation was based on the changes in signal line shape of carbon C_{11} upon the decrease of temperature (Figure S30 and S31), in which the range of temperature was carefully chosen as 263–193 K to avoid the effect of the presence of phase isomers. The resultant data are listed in Table 1.

For molecule **4** possessing more methyl substituents, the decoalescences of amide-NH and pyridonyl protons show up at temperature as high as ca. 213 K (Figure 7). The signal of methyl protons H_{m2} decoalesces at ca. 223 K, indicating slipping caused by the vibration of Tp groups presents expectedly. The decoalescence of Tp signals is hard to identify at 213 K due to the serious broadening but can be clearly observed at 203 K, although those signals could not be precisely assigned in such case. The nonequivalence of two benzene ring with methyl substituents as well as the appearance of phase isomers

gives rise of a very complicated ^{1}H NMR spectrum of **4** at low temperature such as 193 K and 183 K. Nevertheless, the ratio of two phase isomers could be still obtained by integration of splited amide-NH

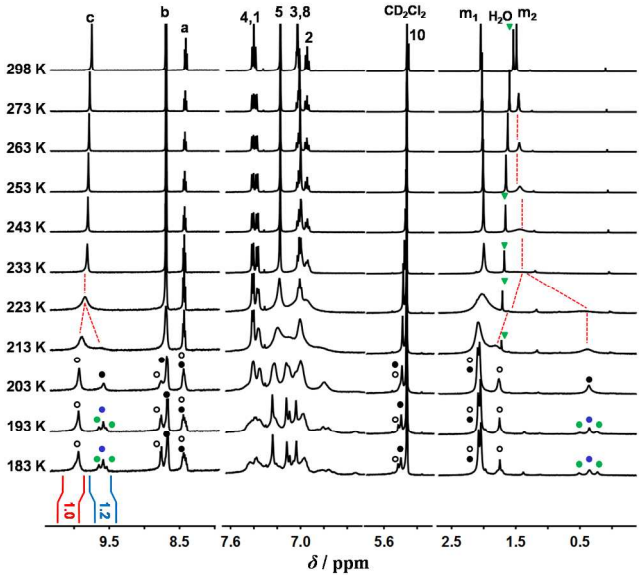

Figure 7. Partial VT ^{1}H NMR spectra (500 MHz) of **4** (2 mM) in CD_2Cl_2. The circles in different colors indicate signals of different set of isomers. The splitting of Tp signals arising from the appearance of phase isomers is hard to distinguish due to the overlap of signals.

signals, which gives that of ca. 1.2:1 rather than 2:1, probably because the *meso* isomers have lower potential energy in the ground state when compared to the *dl* ones (Figure S37 and S38). The changes in signal of methyl protons H_{m1} and H_{m2} upon the decrease of temperature from 263 K to 203 K were used to calculate the thermodynamic parameters for the Tp rotation (Figure S33 and S34). As shown in Table **1**, the values of kinetic parameters in case of **4** are approximate to those of **2**, while the values of **3** are close to those of **1**. This suggests that, in terms of the motion transformation between the two Tp components in the studied systems, combination of unsubstituted Tp group and the one with six methyl substituents might provide similar dynamic property as that of **2**.

Notably, despite both the DFT calculation and VT-NMR experiments indicate a rotation-drove vibration as the most energy-economical way for the motion of **1**, for real molecules in solution, the driving rotator would not be preselected and fixed, and a geared rotation might be still possible to occur (especially at high temperature) if the molecule possess high enough energy for both Tp groups to overcome their respective rotation barriers. Besides, the thermally stimulated motions should occur without direction bias, giving the three-fold symmetry of Tp groups and the absence of any processes of chiral discrimination[8b].

CONCLUSIONS

In summary, we have designed and synthesized a serial of N^2,N^6-bis(triptycene-9-yl)pyridine-2,6-dicarboxamides **1**–**4**, which are derivative from conventional molecular gears. DFT and dynamic NMR experiments have indicated that this kind of molecules possess a different dynamic properties from those of the molecular gears, wherein one triptycene rotator rotates around the C(Tp)–N(amide) bonds while the other one keeps associated rocking vibration through an intermediate slippage process. Enlarging the blades of rotators with methyl substituents gives rise to the raise of the free energy of activation, but would not change the mode of the motion. Our studies thus provide a conceptual approach to design molecular transmission devices those are capable of transforming the mode of motion from rotation to rocking vibration.

EXPERIMENT SECTION:

All starting chemicals were obtained from commercial sources and used without further purification. Anhydrous dichloromethane (DCM) was distilled over calcium hydride (CaH_2) under inert atmosphere. NMR spectra were obtained with a 400, 500 or 600 MHz spectrometer using chloroform-*d* ($CDCl_3$), dichloromethane-d_2 (CD_2Cl_2), methanol-d_4 (CD_3OD) and acetone-d_6 as the solvents. The chemical shift references were as follows: (^{1}H) chloroform-*d*, 7.26 ppm; (^{13}C) chloroform-*d*, 77.16 ppm (chloroform-*d*); (^{1}H) dichloromethane-d_2, 5.32 ppm; dichloromethane-d_2, 53.52 ppm; (^{1}H) methanol-d_4, 3.31 ppm, (^{1}H) acetone-d_5, 2.05 ppm. High resolution mass spectra (EI and ESI) were acquired on GCT, FT-ICR spectrometer. IR spectra were recorded on FT-IR spectrometer with thin KBr disk.

9-nitro-2,3,6,7-tetramethylanthracene (7). To a solution of 2,3,6,7-tetramethylanthracene[37] (190 mg, 0.8 mmol) in CH_2Cl_2 (19 mL), an aqueous HNO_3 solution (20%, 19 mL) was added. The mixture was refluxed for 4 h. The reaction mixture was diluted with water (10 mL) and extracted with CH_2Cl_2 (3×10 mL). The combined organic extracts were dried over Na_2SO_4, then concentrated under reduced pressure. Compound **7** (212 mg, 95%) was obtained as a yellow solid. R_f = 0.6 (petroleum ether (PE)/CH_2Cl_2 = 2/1). Mp = 190–192 °C. IR (KBr): 2918, 2850, 1643, 1531, 1460, 1444, 1384, 1327, 1116, 898 cm^{-1}. ^{1}H NMR (400 MHz, $CDCl_3$), δ = 8.32 (s, 2H), 7.74 (s, 2H), 7.65 (s, 2H), 2.47 (s, 6H), 2.46 (s, 6H); ^{13}C NMR (100 MHz, $CDCl_3$), δ = 139.4, 136.2, 130.1, 127.8, 127.2, 121.8, 120.2, 21.0, 20.3. HRMS (EI-TOF) *m*/*z*: $[M]^+$ calcd for 279.1259 (100%, $C_{18}H_{17}NO_2$), found 279.1263 (100%, 1.3 ppm).

4,5-dimethylbenzenediazonium-2-carboxylate (9). To a mechanically stirred suspension of 4,5-dimethyl anthranilic acid (825 mg, 5 mmol) in ethanol (50 mL) in an ice-water bath was added dropwise concentrated hydrochloric acid (0.63 mL), following the addition of isopentyl nitrite (1.35 mL). After the mixture was stirred for 15 min, diethyl ether (150 mL) was added. Then the reaction mixture was

continued to stir for another 30 min. The product was filtered and washed with diethyl ether to give the product, 975 mg (92%), which was used without further purification.

General Methodology for the Synthesis of Compounds 10–13. The procedure for synthesis of triptycene or derivatives followed as previously reported[38]: Benzynes (**8**[39] or **9**) (7–10 mmol) was added in portions to a mixture of 9-nitroanthracene or its derivative **7** (1 mmol) and 1,2-epoxypropane (2 mL) in dichloroethane (30 mL) for refluxing 24 h. The reaction mixture was concentrated under reduced pressure. Then the resultant solid was washed with methanol. The residue was purified by silica gel column chromatography.

9-nitrotriptycene (10). Purification by silica gel column chromatography (PE/CH_2Cl_2 = 3/1) to give compound **10** (137 mg, 46%) as a white solid. R_f = 0.5 (PE/CH_2Cl_2 = 3/1). Mp = 246–248 °C. IR (KBr): 3072, 3038, 2968, 1543, 1459, 1446, 1365, 1295, 1156, 872, 803, 752, 620 cm^{-1}. ^1H NMR (400 MHz, $CDCl_3$), δ = 7.67-7.71 (m, 3H), 7.42-7.46 (m, 3H), 7.09-7.14 (m, 6H), 5.42 (s, 1H); ^{13}C NMR (100 MHz, CDCl3), δ = 143.8, 140.4, 126.9, 125.8, 123.7, 122.1, 96.9, 54.0. HRMS (EI-TOF) (*m*/*z*) $[M]^+$ calcd for 299.0946 (100%, $C_{20}H_{13}NO_2$), found 299.0950 (100%, 1.2 ppm). Lit.[26a] Yield: 33%; ^1H NMR ($CDCl_3$), δ = 7.68 (m, 3H), 7.44 (m, 3H), 7.07-7.15 (m, 6H), 5.41 (s, 1H).

2,3,6,7,14,15-hexamethyl-9-nitrotriptycene (11). Purification by silica gel column chromatography (PE/CH_2Cl_2 = 3/1) to give compound **11** (27 mg, 7%) as a white solid. R_f = 0.5 (PE/CH_2Cl_2 = 3/1). Mp = 258–260 °C. IR (KBr): 3010, 2958, 2920, 2853, 1548, 1465, 1384, 1362, 1271, 866, 809, 604 cm^{-1}. ^1H NMR (400 MHz, $CDCl_3$), δ = 7.41 (s, 3H), 7.16 (s, 3H), 5.17 (s, 1H), 2.17 (s, 9H), 2.16 (s, 9H); ^{13}C NMR (100 MHz, $CDCl_3$), δ = 141.9, 138.6, 137.1, 135.5, 134.7, 133.4, 124.7, 123.0, 122.8, 96.7, 52.7,

19.8, 19.5. HRMS (EI-TOF) (*m*/*z*) $[M]^+$ calcd for 383.1885 (100%, $C_{26}H_{25}NO_2$), found 383.1884 (100%, -0.3 ppm).

2,3-dimethyl-9-nitrotriptycene (12). Purification by silica gel column chromatography (PE/CH_2Cl_2 = 3/1) to give compound **12** (115 mg, 35%) as a white solid. R_f = 0.5 (PE/CH_2Cl_2 = 3/1). Mp = 235–238 °C. IR (KBr): 3067, 2963, 2921, 1545, 1460, 1383, 1364, 1292, 868, 805, 760, 745, 662 cm^{-1}. ^1H NMR (400 MHz, $CDCl_3$): δ = 7.65-7.67 (m, 2H), 7.45 (s, 1H), 7.40-7.42 (m, 2H), 7.23 (s, 1H), 7.08-7.10 (m, 4H), 5.33 (s, 1H), 2.19 (s, 3H), 2.18 (s, 3H); ^{13}C NMR (100 MHz, $CDCl_3$), δ = 144.1, 140.7, 138.0, 135.1, 141.3, 133.8, 126.8, 125.6, 125.0, 123.5, 123.3, 121.9, 96.9, 53.6, 19.9, 19.5. HRMS (EI-TOF) (*m*/*z*) $[M]^+$ calcd for 327.1259 (100%, $C_{22}H_{17}NO_2$), found 327.1256 (100%, -1.0 ppm).

2,3,6,7-tetramethyl-9-nitrotriptycene (13). Purification by silica gel column chromatography (PE/CH_2Cl_2 = 3/1) to give compound **13** (53 mg, 15%) as a white solid. R_f = 0.5 (PE/CH_2Cl_2 = 3/1). Mp = 232–235 °C. IR (KBr):3065, 3038, 2918, 1634, 1548, 1463, 1383, 1361, 1272, 756, 613 cm^{-1}. ^1H NMR (400 MHz, $CDCl_3$), δ = 7.64 (t, 1H, J = 4.2 Hz), 7.44 (s, 2H), 7.38 (t, 1H, J = 4.2 Hz), 7.20 (s, 2H), 7.06-7.08 (m, 2H), 5.26 (s, 1H), 2.18 (s, 6H), 2.17 (s, 6H); ^{13}C NMR (100 MHz, $CDCl_3$), δ = 144.4, 141.7, 141.0, 138.3, 134.9, 133.7, 126.7, 125.6, 124.9, 123.3, 123.2, 121.8, 96.8, 53.2, 19.9, 19.5. HRMS (EI-TOF) (*m*/*z*) $[M]^+$ calcd for 355.1572 (100%, $C_{24}H_{21}NO_2$), found 355.1570 (100%, -0.6 ppm).

General Methodology for the Synthesis of Compounds 14–17. Reduction of compounds **10**–**13** with $SnCl_2$/HCl according to the procedure reported in the literature[27] afforded compounds **14**–**17** with good yields.

9-triptycylamine (14). Compound **14** was obtained as a white solid in 92% yield. R_f = 0.3 (PE/ethyl acetate = 2/1). Mp = 212–214 °C. IR (KBr): 3442, 3385, 3067, 2951, 1617, 1455, 1296, 1130, 749,

633 cm^{-1}. ^1H NMR (400 MHz, $CDCl_3$), δ = 7.49 (d, 3H, J = 7.3 Hz), 7.40 (d, 3H, J = 6.9 Hz), 7.01-7.09 (m, 6H), 5.43 (s, 1H), 2.61 (br, 2H); ^{13}C NMR (100 MHz, $CDCl_3$), δ = 146.8, 145.1, 125.4, 125.2, 123.4, 119.5, 64.3, 53.4. HRMS (ESI-FT-ICR) $[M+H]^+$ calcd for 270.127726 (100%, $C_{20}H_{16}N$), found 270.127790 (100%, -0.2 ppm). Lit.[26a] Yield: 91%; ^1H NMR ($CDCl_3$), δ = 7.48 (m, 3H), 7.38 (m, 3H), 7.06 (m, 3H), 7.01 (m, 3H), 5.409 (s, 1H), 2.607 (br, 2H).

2,3,6,7,14,15-hexamethyl-9-triptycylamine (15). Compound **15** was obtained as a white solid in 90% yield. R_f = 0.3 (PE/ethyl acetate = 2/1). Mp = 290–292 °C. IR (KBr): 3439, 3373, 3004, 2957, 2917, 2854, 1626, 1465, 1383, 1284, 996, 865, 622 cm^{-1}. ^1H NMR (400 MHz, $CDCl_3$), δ = 7.21 (s, 3H), 7.13 (s, 3H), 5.19 (s, 1H), 2.56 (br, 2H), 2.16 (s, 9H), 2.14 (s, 9H); ^{13}C NMR (100 MHz, $CDCl_3$), δ = 144.8, 143.2, 132.9, 132.6, 124.7, 120.8, 63.4, 52.0, 19.7, 19.5. HRMS (ESI-FT-ICR) (m/z) $[M+H]^+$ calcd for 354.221626 (100%, $C_{26}H_{28}N$), found 354.221764 (100%, -0.4 ppm).

2,3-dimethyl-9-triptycylamine (16). Compound **16** was obtained as a white solid in 92% yield. R_f = 0.3 (PE/ethyl acetate =2/1). Mp = 216–218 °C. IR (KBr): 3375, 3319, 3000, 2957, 2915, 1629, 1456, 1383, 1269, 1025, 913, 884, 806, 759, 739, 621 cm^{-1}. ^1H NMR (400 MHz, CD_3OD), δ = 7.48 (d, 2H, J = 6.8 Hz), 7.34 (d, 2H, J = 6.8 Hz), 7.27 (s, 1H), 7.15 (s, 1H), 6.96-7.04 (m, 4H), 5.35 (s, 1H), 2.20 (s, 3H), 2.17 (s, 3H); ^{13}C NMR (100 MHz, $CDCl_3$), δ = 147.2, 145.4, 144.3, 142.8, 133.2, 132.9, 125.3, 125.1, 123.3, 121.1, 119.4, 119.3, 64.1, 52.9, 19.8, 19.6. HRMS (ESI-FT-ICR) (m/z) $[M+H]^+$ calcd for 298.159026 (100%, $C_{22}H_{20}N$), found 298.159170 (100%, -0.5 ppm).

2,3,6,7-tetramethyl-9-triptycylamine (17). Compound 17 was obtained as a white solid in 90% yield. R_f = 0.3 (PE/ethyl acetate =2/1). Mp = 212–214 °C. IR (KBr): 3444, 3374, 3007, 2921, 2852, 1627, 1454, 1383, 1261, 1021, 803, 621 cm^{-1}. ^1H NMR (400 MHz, $CDCl_3$), δ = 7.43 (d, 2H, J = 7.2 Hz), 7.33

(d, 2H, J = 7.2 Hz), 7.24 (s, 1H), 7.16 (s, 1H), 6.96-7.05 (m, 2H), 5.27 (s, 1H), 2.56 (br, 2H), 2.18 (s, 3H), 2.16 (s, 3H); ^{13}C NMR (100 MHz, $CDCl_3$), δ = 147.4, 145.7, 144.6, 143.0, 133.0, 132.8, 125.3, 125.0, 124.9, 123.1, 120.9, 119.1, 63.8, 52.5, 19.8, 19.5. HRMS (ESI-FT-ICR) (m/z) $[M+H]^+$ calcd for 326.190326 (100%, $C_{24}H_{24}N$), found 326.190486 (100%, -0.5 ppm).

Compound 1. A mixture of **14** (323 mg, 1.2 mmol), 2,6-pyridinedicarboxylic acid chloride (102 mg, 0.5 mmol), and *N*,*N*-diisopropylethylamine (DIEA, 0.66 mL, 4 mmol) in dry CH_2Cl_2 (20 mL) was stirred under N_2 atmosphere for overnight. The solution was concentrated under reduced pressure. The residue was purified by silica gel column chromatography (CH_2Cl_2/ethyl acetate = 200/1) to afford **1** as a white solid (187 mg, 56%). R_f = 0.7 (CH_2Cl_2/ethyl acetate = 30/1). Mp > 300 °C. IR (KBr): 3410 (NH), 3062, 3022, 2925, 2856, 1695 (C=O), 1510, 1451, 1250, 991, 748, 624 cm^{-1}. ^{1}H NMR (400 MHz, $CDCl_3$), δ = 9.61 (s, 2H), 8.82 (d, 2H, J = 7.8 Hz), 8.37 (t, 1H, J = 7.8 Hz), 7.42-7.48 (m, 12H), 7.03-7.06 (m, 6H), 6.93-6.97 (m, 6H), 5.50 (s, 2H); ^{13}C NMR (100 MHz, $CDCl_3$), δ = 163.3, 149.8, 144.3, 142.5, 140.0, 126.7, 125.9, 125.1, 123.9, 120.9, 66.9, 53.8. HRMS (ESI-FT-ICR) (m/z) $[M+H]^+$ calcd for 670.2495 (100%, $^{12}C_{47}H_{32}N_3O_2$); 671.2528 ($^{12}C_{46}{}^{13}C_1H_{32}N_3O_2$); found 670.2509 (100%, 2.1 ppm), 671.2542 (60%, 2.1 ppm).

Compound 2. A mixture of 2,6-Pyridinedicarboxylic acid (10.2 mg, 0.05 mmol), and benzotriazol-1-yl-oxytripyrrolidinophosphonium hexafluorophosphate (PyBOP, 62.4 mg, 0.12 mmol), 4-dimethylaminopyridine (DMAP, 24 mg, 0.2 mmol) in anhydrous DMF (20 mL) was stirred for 30 min. Then a solution of compound **16** (35 mg, 0.1 mmol) in anhydrous DMF was added and the reaction mixture was refluxed under N_2 atmosphere for 2 days. The solution was concentrated under reduced pressure. Purification by silica gel column chromatography (CH_2Cl_2/ethyl acetate = 200/1) to afford **2** as

a white solid (20 mg, 51%). R_f = 0.7 (CH_2Cl_2/ethyl acetate = 30/1). Mp > 300 °C. IR (KBr): 3412 (NH), 3075, 2925, 1701 (C=O), 1518, 1459, 1008, 849, 624 cm^{-1}. ^1H NMR (400 MHz, $CDCl_3$), δ = 9.86 (s, 2H), 8.77 (d, 2H, J = 7.6 Hz), 8.39 (t, 1H, J = 7.6 Hz), 7.12 (s, 6H), 7.06 (s, 6H), 5.18 (s, 2H), 2.03 (s, 18H), 1.59 (s, 18H); ^{13}C NMR (100 MHz, $CDCl_3$), δ = 163.2, 150.0, 142.4, 140.8, 140.3, 133.3, 132.7, 125.7, 124.9, 122.0, 66.0, 52.4, 19.4, 19.1. HRMS (ESI-FT-ICR) (m/z) $[M+H]^+$ calcd for 838.4373 (100%, $^{12}C_{59}H_{56}N_3O_2$); 839.4406 ($^{12}C_{58}{}^{13}C_1H_{56}N_3O_2$); found 838.4369 (100%, 0.0 ppm), 839.4467 (60%, 7.3 ppm).

Compound 3. Compound **3** was synthesized in a similar way to that described for **1** and obtained as a white solid in 52% yield. R_f = 0.7 (CH_2Cl_2/ethyl acetate = 30/1). Mp > 300 °C. IR (KBr): 3410 (NH), 3069, 2921, 1700 (C=O), 1518, 1459, 1383, 756, 619 cm^{-1}. ^1H NMR (400 MHz, Acetone-d_6), δ = 9.97 (s, 2H), 8.67 (d, 2H, J = 7.2 Hz), 8.56 (t, 1H, J = 7.2 Hz), 7.49-7.55 (m, 8H), 7.24 (s, 1H), 7,15 (s, 1H), 7.03 (t, 4H, J = 7.2 Hz), 6.93 (t, 4H, J = 7.2 Hz), 5.61 (s, 2H), 2.01 (s, 6H), 1.32 (s, 6H); ^{13}C NMR (100 MHz, $CDCl_3$), δ = 163.4, 149.9, 144.5, 142.7, 142.1, 140.4, 140.3, 133.7, 133.2, 126.2, 125.8, 125.4, 125.1, 123.7, 121.6, 121.1, 66.6, 53.3, 19.4, 18.8. HRMS (ESI-FT-ICR) (m/z) $[M+H]^+$ calcd for 726.3121 (100%, $^{12}C_{51}H_{40}N_3O_2$); 727.3154 ($^{12}C_{50}{}^{13}C_1H_{56}N_3O_2$); found 726.3122 (100%, 0.1 ppm), 727.3209 (60%, 7.6 ppm).

Compound 4. Compound **4** was synthesized in a similar way to that described for **1** and obtained as a white solid in 47% yield. R_f = 0.7 (CH_2Cl_2/ethyl acetate = 30/1). Mp > 300 °C. IR (KBr): 3400 (NH), 3068, 3005, 2922, 2853, 1701 (C=O), 1519, 1459, 1384, 1263, 842, 754, 619 cm^{-1}. ^1H NMR (400 MHz, $CDCl_3$), δ = 9.82 (s, 2H), 8.76 (d, 2H, J = 8.0 Hz), 8.39 (t, 1H, J = 8.0 Hz), 7.36-7.42 (m, 4H), 7.15 (s, 4H), 7.03 (s, 4H), 6.91-7.01 (m, 4H), 5.27 (s, 2H), 2.02 (s, 12H), 1.26 (s, 12H); ^{13}C NMR (100 MHz,

$CDCl_3$): δ = 163.3, 149.9, 144.6, 142.9, 142.2, 140.6, 140.4, 133.5, 132.9, 125.9, 125.7, 125.2, 124.9, 123.4, 121.8, 121.4, 66.3, 52.9, 19.4, 18.8. HRMS (ESI-FT-ICR) (*m*/*z*) $[M+H]^+$ calcd for 782.3747 (100%, $^{12}C_{55}H_{48}N_3O_2$); 783.3780 ($^{12}C_{54}{}^{13}C_1H_{48}N_3O_2$); found 782.3754 (100%, 0.9 ppm), 783.3779 (60%, -1.4 ppm).

ACKNOWLEDGMENT. We thank the National Natural Science Foundation of China (21125205 and 21332008) for financial support.

SUPPORTING INFORMATION. X-ray crystallographic data as well as CIF file of **1**–**4**; VT NMR spectra and Eyring plot analyses of **1**–**4**; computational details; ^{1}H NMR, ^{13}C NMR and 2D NMR spectra; videos of rotational isomerization of **1** and **2**. This material is available free of charge via the Internet at http://pubs. acs. org.

REFERENCES

(1) Sauvage, J. -P.; Amendola,V.; Ballardini, R.; Balzani, V.; Credi, A.; Fabbrizzi, L.; Gandolfi, M. T.; Gimzewski, J. K.; Gómez-Kaifer, M.; Joachim, C.; Kaifer, A. E.; Katz, E.; Kelly, T. R.; Liu, J.; Mangano, C.; Pallavicini, P.; Pease, A. R.; Raehm, L.; Sano, M.; Sauvage, J. -P.; Sestelo, J. P.; Shipway, A. N.; Stoddart, J. -F. ; Venturi, M.; Willner, I., Eds. *Molecular Machines and Motors*; Springer: Berlin, Germany, 2001.

(2) (a) Balzani, V.; Credi, A.; Raymo, F. M.; Stoddart, J. F. *Angew. Chem. Int. Ed*. **2000**, 39, 3348–3391. (b) Kottas, G. S.; Clarke, L. I.; Horinek, D.; Michl, J. *Chem. Rev.* **2005**, 105, 1281–1376. (c) Browne, W. R.; Feringa, B. L. *Nat. Nanotechnol*. **2006**, 1, 25–35. (d) Kay, E. R.; Leigh, D.A.; Zerbetto, F. *Angew. Chem. Int. Ed*. **2007**, 46, 72–191. (e) Michl, J.; Sykes, E. C. H. *Nano.*

Focus. **2009**, 3, 1042–1048.

(3) (a) Kao, C. Y.; Hsu, Y. T.; Lu, H. F.; Chao, I.; Huang, S. L.; Lin, Y. C.; Sun, W. T.; Yang, J. S. *J. Org. Chem.* **2011**, 76, 5782–5792. (b) Chen, G.; Zhao, Y. *Org. Lett*. **2014**, 16, 668–671.

(4) (a) Gan, Q.; Ferrand, Y.; Bao, C. Y.; Kauffmann, B.; Grélard, A.; Jiang, H.; Huc, I. *Science.* **2011**, 331, 1172–1175. (b) Blanco, V.; Leigh, D. A.; Marcos, V.; Morales-Serna, J. A.; Nussbaumer, A. L. *J. Am. Chem. Soc*. **2014**, 136, 4905−4908.

(5) (a) Kelly, T. R.; Michael, C.; Bowyer, K.; Vijaya, B.; David, B.; Albert, G.; Fengrui, L.; Min, H. K.; Michael, P. J. *J. Am. Chem. Soc.* **1994**, 116, 3657–3658. (b) Nikitin, K.; Bothe, C.; Müller-Bunz, H.; Ortin, Y.; McGlinchey M. J. *Organometallics*. **2012**, 31, 6183–6198.

(6) (a) Bedard, T. C.; Moore, J. S. *J. Am. Chem. Soc.* **1995**, 117, 10662–10671. (b) Guenet, A.; Graf, E.; Kyritsakas, N.; Hosseini, M. W. *Inorg. Chem.* **2010**, 49, 1872–1883. (c) Lang, T.; Graf, E.; Kyritsakas, N.; Hosseini, M. W. *Chem. Eur. J.* **2012**, 18, 10419–10426. (d) Zigon, N.; Larpent, P.; Jouaiti, A.; Kyritsakas, N.; Hosseini, M. W. *Chem. Commun*. **2014**, 50, 5040–5042.

(7) Kelly, T. R. *Acc. Chem. Res*. **2001**, 34, 514–522.

(8) (a) Kelly, T. R.; Silva, D. H.; Silva, R. A. *Nature.* **1999**, 401, 150–152. (b) Koumura, N.; Zijlstra, R. W. J.; Richard, A. D.; Harada, N.; Feringa, B. L. *Nature.* **1999**, 401, 152–155. (c) Fletcher, S. P.; Dumur, F.; Pollard, M. M.; Feringa, B. L. *Science*. **2005**, 310, 80–82. (d) Wang, J. B.; Feringa, B. L. *Science*. **2011**, 331, 1429–1432.

(9) Khuong, T. V.; Nunez, J. E.; Godinez, C. E.; Garcia-Garibay, M. A. *Acc. Chem. Res*. **2006**, 39, 413–422.

(10) (a) Dominguez, Z.; Dang, H.; Strouse, M. J.; Garcia-Garibay, M. A. *J. Am. Chem. Soc.* **2002**, 124, 2398–2399. (b) Nawara, A. J.; Shima, T.; Frank, H.; Gladysz, J. A. *J. Am. Chem. Soc*. **2006**, 128, 4962–4963. (c) Jarowski, P. D.; Houk, K. N.; Garcia-Garibay, M. A. *J. Am. Chem. Soc.* **2007**, 129, 3110–3117. (d) Setaka, W.; Yamaguchi, K. *J. Am. Chem. Soc.* **2013**, 135, 14560−14563. (e) Commins, P.; Garcia-Garibay, M. A. *J. Org. Chem.* **2014**, 79, 1611–1619.

(11) (a) Hounshell, W. D.; Johnson, C. A.; Guenzi, A.; Cozzi, F.; Mislow, K. *Proc. Natl. Acad. Sci. USA.* **1980**, 77, 6961–6964. (b) Cozzi, F.; Guenzi, A.; Johnson, C. A.; Mislow, K.; Hounshell, W. D.; Blount, J. F. *J. Am. Chem. Soc.* **1981**, 103, 957–958. (c) Johnson, C. A.; Guenzi, A.; Mislow, K. *J. Am. Chem. Soc.* **1981**, 103, 6240–6242. (d) Biirgi, H. B.; Hounshell, W. D.; Nachbar, R. B., Jr.; Mislow, K. *J. Am. Chem. Soc.* **1983**, 105, 1427–1438.

(12) (a) Kawada, Y.; Iwamura, H. *J. Org. Chem.* **1980**, 45, 2547–2548. (b) Kawada, Y.; Iwamura, H. *J. Am. Chem. Soc.* **1981**, 103, 958–960. (c) Kawada, Y.; Iwamura, H. *Tetra. Lett.* **1981**, 22, 1533–1536. (d) Iwamura, H.; Ito, T.; Ito, H.; Toriumi, K.; Kawada, Y.; Osawa, E.; Fujiyoshi, T.; Jaime, C. *J. Am. Chem. Soc.* **1984**, 106, 4712–4717.

(13) (a) Johnson, C. A.; Guenzi, A.; Nachbar, R. B.; Jr., Blount, J.F.; Wennerstrom, O.; Mislow, K. *J. Am. Chem. Soc.* **1982**, 104, 5163–5168. (b) Guenzi, A,; Johnson, C. A.; Cozzi, F.; Mislow, K. *J. Am. Chem. Soc.* **1983**, 105, 1438–1448. (c) Kawada, Y.; Iwamura, H. *J. Am. Chem. Soc.* **1983**, 105, 1449–1459.

(14) Kawada, Y.; Yamazaki, H.; Koga, G.; Murata, S.; Iwamura, H. *J. Org. Chem.* **1986**, 51, 1472–1477.

(15) Iwamura, H.; Mislow, K. *Acc. Chem. Res.* **1988**, 21, 175–182.

(16) (a) Koga, N.; Kawada, Y.; Iwamura, H. *J. Am. Chem. Soc.* **1983**, 105, 5498–5499. (b) Koga, N.; Kawada, Y.; Iwamura, H. *Tetrahedron*. **1986**, 42, 1679–1686. (c) Chance, J. M.; Geiger, J.H.;

Mislow, K. *J. Am. Chem. Soc.* **1989**, 111, 2327–2329. (d) Chance, J.M.; Geiger, J.H. Okamoto, Y.; Aburatani, R.; Mislow. K. *J. Am. Chem. Soc*. **1990**, 112, 3540–3547.

(17) Kawada, Y.; Sakai, H.; Oguri, M.; Kgga, G. *Tetra. Lett.* **1994**, 35, 139–142.

(18) Setaka, W.; Nirengi ,T.; Kabuto, C.; Kira, M. *J. Am. Chem. Soc*. **2008**, 130, 15762–15763.

(19) Frantz, D. K.; Baldridge, K. K.; Siegel, J. S. *Chimia.* **2009**, 63, 201–204.

(20) Frantz, D. K.; Linden, A.; Baldridge, K. K.; Siegel, J. S. *J. Am. Chem. Soc.* **2012**, 134, 1528–1535.

(21) Bryan, J. C.; Sachleben, R. A.; Gakh, A. A.; Bunick, G. J. *J. Chem. Cryst*. **1999**, 29, 513–521.

(22) (a) Dolain, C., Maurizot, V., Huc, I. *Angew. Chem. Int. Ed*. **2003**, 42, 2738–2740. (b) Haldar, D.; Jiang, H.; Léger, J. M.; Huc, I. *Tetra.* **2007**, 63, 6322–6330. (c) Monchaud, D., Yang, P., Lacroix, L., Teulade-Fichou M. P., Mergny, J. *Angew. Chem. Int. Ed*. **2008**, 47, 4858–4861.

(23) Morse, J. K. *Proc. Natl. Acad. Sci. USA*., **1927**, 13, 789–793.

(24) Stevens, A. M.; Richards, C. J. *Tetra. Lett.* **1997**, 38, 7805–7808.

(25) (a) Friedman, L.; Logullo, F. M. *J. Org. Chem.* **1969**, 34, 3089–3092. (b) Klanderman, B. H.; Criswell. T. R. *J. Org. Chem*. **1969**, 34, 3426–3430.

(26) (a) Yamamoto, G.; Higuchi, H.; Yonebayashi, M.; Nabeta, Y.; Ojima J. *Tetrahedron*. **1996**, 52, 12409–12420. (b) Yamamoto, G.; Agawa, C.; Ohno, T.; Minoura, M.; Mazaki, Y. *Bull. Chem. Soc. Jpn.* **2003**, 76, 1801–1811.

(27) Theilacker, W.; Beyer, K. -H. *Chem. Ber.* **1961**, 94, 2968–2977.

(28) Sala, M.; Kirkby, O. M.; Guérin, S.; Fielding, H. H. *Phys. Chem. Chem. Phys.* **2014**, 16, 3122–3133..

(29) Bobadova-Parvanova, P., Jackson, K. A., Srinivas, S., Horoi, M.; KÖhler, C.; Seifert, G. *J. Chem. Phys.* **2002**, 116, 3576–3587.

(30) Frisch, M. J.; Trucks, G. W.; Schlegel, H. B.; Scuseria, G. E.; Robb, M. A.; Cheeseman, J. R.; Montgomery, J. A., Jr.; Vreven, T.; Kudin, K. N.; Burant, J. C.; Millam, J. M.; Iyengar, S. S.; Tomasi, J.; Barone, V.; Mennucci, B.; Cossi, M.; Scalmani, G.; Rega, N.; Petersson, G. A.; Nakatsuji, H.; Hada, M.; Ehara, M.; Toyota, K.; Fukuda, R.; Hasegawa, J.; Ishida, M.; Nakajima, T.; Honda, Y.; Kitao, O.; Nakai, H.; Klene, M.; Li, X.; Knox, J. E.; Hratchian, H. P.; Cross, J. B.; Adamo, C.; Jaramillo, J.; Gomperts, R.; Stratmann, R. E.; Yazyev, O.; Austin, A. J.; Cammi, R.; Pomelli, C.; Ochterski, J. W.; Ayala, P. Y.; Morokuma, K.; Voth, G. A.; Salvador, P.; Dannenberg, J. J.; Zakrzewski, V. G.; Dapprich, S.; Daniels, A. D.; Strain, M. C.; Farkas, O.; Malick, D. K.; Rabuck, A. D.; Raghavachari, K.; Foresman, J. B.; Ortiz, J. V.; Cui, Q.; Baboul, A. G.; Clifford, S.; Cioslowski, J.; Stefanov, B. B.; Liu, G.; Liashenko, A.; Piskorz, P.; Komaromi, I.; Martin, R. L.; Fox, D. J.; Keith, T.; Al-Laham, M. A.; Peng, C. Y.; Nanayakkara, A.; Challacombe, M.; Gill, P. M. W.; Johnson, B.; Chen, W.; Wong, M. W.; Gonza´lez, C.; Pople, J. A. Gaussian03 Revision D.02; Gaussian, Inc.: Pittsburgh, PA, 2004.

(31) (a) Roussel, C.; Vanthuyne, N.; Bouchekara, M.; Djafri, A.; Elguero, J.; Alkorta, I. *J. Org. Chem.* **2008**, 73, 403−411. (b) Dial, B. E.; Pellechia, P. J.; Smith, M. D.; Shimizu, K. D. *J. Am. Chem. Soc.* **2012**, 134, 3675–3678.

(32) (a) Zhang, Z. Y.; Wu, Y. S.; Tang, K. C.; Chen, C. L.; Ho, J. W.; Su, J. H.; Tian, H.; Chou P. T. *J. Am. Chem. Soc*. **2015**, 137, 8509–8520. (b) Huang, W.; Sun, L.; Zheng, Z. W.; Su, J. H.; Tian, H. Chem. Commun. **2015**, 51, 4462–4464.

(33) Rohonczy, J. *DNMR Line shape Analysis, Software Manual*, version 1.1; Bruker BioSpin GmbH: Rheinstetten, 2007.

(34) For examples that performing VT ^{13}C NMR to avoid the analysis of complicated VT ^{1}H NMR spectra for thermodynamic parameters, see: (a) Yang, J. S.; Huang, Y. H.; Ho, J. H.; Sun, W. T.; Huang, H. H.; Lin, Y. C.; Huang, S. J.; Huang, S. L.; Lu, H. F.; Chao, I. *Org. Lett.* **2008**, 10,

2279–2282. (b) Sun, W. T.; Huang, Y. T.; Huang, G. J.; Lu, H. F.; Chao, I.; Huang, S. L.; Huang, S. J.; Lin, Y. C.; Ho, J. H.; Yang, J. S. *Chem. Eur. J.* **2010**, 16, 11594–11604. (c) Sun, W. T.; Huang, S. L.; Yao, H, H.; Chen, I. C.; Lin, Y. C.; Yang, J. S. *Org. Lett.* **2012**, 14, 4154–4157.

(35) The free energy of activation ($\Delta G^{\#}$), the enthalpy ($\Delta H^{\#}$) and entropy ($\Delta S^{\#}$) were derived from the Eyring plots. See (a) Sandstrom, J. *Dynamic NMR Spectroscopy*. London: Academic Press, 1982. (b) Zimmer, K. D.; Shoemaker, R.; Ruminski, R. R. *Inorg. Chim. Acta.* **2006**, 359, 1478–1484.

(36) Similar phenomenon has been also observed in other molecular rotary system. For example, see Chen, Y. C.; Sun, W. T.; Lu, H. F.; Chao, I.; Huang, G. J.; Lin, Y.C.; Huang, S. L.; Huang, H. H.; Lin, Y. D.; Yang, J. S. *Chem. Eur. J.* **2011**, 17, 1193–1200.

(37) 2,3,6,7-tetramethylanthracene was synthesized according to the procedures reported in following literatures: (a) Hess, H. J.; Cronin, T. H.; Scriabine, A. *J. Med. Chem.* **1968**, 11, 130–136. (b) Bender, D.; Mullen, K. *Chem. Ber.* **1988**, 121, 1187–1197. (c) Godinez, C. E.; Zepeda, G.; Mortko, C. J.; Dang, H.; Garcia-Garibay, M. A. *J. Org. Chem*. **2004**, 69, 1652–1662.

(38) Zhu, X. Z.; Chen, C. F. *J. Am. Chem. Soc.* **2005**, 127, 13158–13159.

(39) Compound **8** was obtained according to the procedure reported in literature 25b, and the compound was used directly without further purification.